Faculty Scholarship

2015

Sox9 Inhibits -Trcp-Mediated Protein Degradation To Promote Nuclear Gli1 Expression And Cancer Stem Cell Properties

W. Deng

D. B. Vanderbilt

C.-C. Lin

K. H. Martin

K. M. Brundage

See next page for additional authors

Follow this and additional works at: https://researchrepository.wvu.edu/faculty_publications

Authors

W. Deng, D. B. Vanderbilt, C.-C. Lin, K. H. Martin, K. M. Brundage, and J. M. Ruppert

The Company *of*
Biologists

RESEARCH ARTICLE

SOX9 inhibits β-TrCP-mediated protein degradation to promote nuclear GLI1 expression and cancer stem cell properties

Wentao Deng[1,2,*], Daniel B. Vanderbilt[3,*], Chen-Chung Lin[1,2], Karen H. Martin[2], Kathleen M. Brundage[2] and J. Michael Ruppert[1,2,3,‡]

ABSTRACT

The high mobility group box protein SOX9 and the GLI1 transcription factor play protumorigenic roles in pancreatic ductal adenocarcinoma (PDA). In Kras transgenic mice, each of these factors are crucial for the development of PDA precursor lesions. SOX9 transcription is directly regulated by GLI1, but how SOX9 functions downstream of GLI1 is unclear. We observed positive feedback, such that SOX9-deficient PDA cells have severely repressed levels of endogenous GLI1, attributed to loss of GLI1 protein stability. SOX9 associated with the F-box domain of the SKP1/CUL1/F-box (SCF) E3 ubiquitin ligase component, β-TrCP (also known as F-box/WD repeat-containing protein 1A), and suppressed its association with SKP1 and GLI1, a substrate of SCF-β-TrCP. SOX9 also tethered β-TrCP within the nucleus and promoted its degradation. SOX9 bound to β-TrCP through the SOX9 C-terminal PQA/S domain that mediates transcriptional activation. Suppression of β-TrCP in SOX9-deficient PDA cells restored GLI1 levels and promoted SOX9-dependent cancer stem cell properties. These studies identify SOX9–GLI1 positive feedback as a major determinant of GLI1 protein stability and implicate β-TrCP as a latent SOX9-bound tumor suppressor with the potential to degrade oncogenic proteins in tumor cells.

KEY WORDS: Pancreatic ductal adenocarcinoma, SOX9, GLI1, β-TrCP

INTRODUCTION

The evolution of metazoans required new strategies for proper regulation of cell fate, including intercellular signaling, signal reception and signal transduction, processes in which transcription factors play crucial roles (Nusse, 2003; Weinberg, 2007). Central to cancer etiology is the dysregulation of cell fate, often through genetic changes that impinge on transcription factor signaling (Taipale and Beachy, 2001; Kalderon, 2002). GLI1, a member of the GLI family of zinc finger transcription factors, is a central regulator of cell fate that is deregulated in diverse tumor types (Lauth and Toftgård, 2007; Ruiz i Altaba et al., 2007; Stecca and Ruiz i Altaba, 2010; Morris et al., 2010; Hui and

[1]The Department of Biochemistry, West Virginia University, Morgantown, West Virginia 26506. [2]The Mary Babb Randolph Cancer Center, West Virginia University, West Virginia 26506. [3]Program in Cancer Cell Biology, West Virginia University, Morgantown, West Virginia 26506.
*These authors contributed equally to this work

‡Author for correspondence (mruppert@hsc.wvu.edu)

Angers, 2011). Increased levels of GLI1 mRNA and protein can result from genetic inactivation of tumor suppressors, such as the Hedgehog pathway receptor Patched1 (PTCH1), or mutational activation of factors such as Smoothened (SMO). GLI1 signaling impacts on multiple cancer-relevant cellular processes, promoting dedifferentiation, the generation of cancer stem cells (CSCs), tumor progression and metastasis. In addition, GLI1 can directly induce the transcription of its own mRNA through a well-characterized autoregulatory feedback, and therefore *GLI1* mRNA levels often reflect the overall GLI transactivation capacity (Dai et al., 1999; Vokes et al., 2007).

Pancreatic ductal adenocarcinoma (PDA) is an aggressively metastatic tumor type that is often diagnosed at a later clinical stage (Koorstra et al., 2008; Feig et al., 2012). Although GLI1 is expressed in both epithelial PDA cells and stromal cells, a cell autonomous role within carcinoma cells appears central to the pathogenesis of this disease (Feldmann et al., 2007; Nolan-Stevaux et al., 2009; Tian et al., 2009; Lauth et al., 2010). Indeed, suppression of GLI1 in human PDA cells leads to loss of malignant properties (Ji et al., 2007; Feldmann et al., 2007; Nolan-Stevaux et al., 2009). In a *Kras*-dependent mouse model of PDA, either Cre-mediated excision of *Gli1* or expression of a dominant-negative GLI factor suppresses tumorigenesis, including the outgrowth of precursor lesions termed pancreatic intraepithelial neoplasia (PanIN) (Rajurkar et al., 2012; Mills et al., 2013). Conversely, enforced expression of an active GLI factor in pancreatic epithelial cells promotes tumorigenesis in mice (Pasca di Magliano et al., 2006). In the canonical Hedgehog–GLI pathway, GLI activity is dependent upon signaling by Hedgehog through PTCH1 and SMO, whereas in PDA cells GLI1 is instead maintained by activated KRAS (Hingorani et al., 2005; Pasca di Magliano et al., 2006; Ji et al., 2007; Nolan-Stevaux et al., 2009; Tian et al., 2009; Lauth et al., 2010).

The protein stability of GLI1 is regulated by two E3 ubiquitin ligases, the Skp/Cul/F-box complex SCF[β-TrCP] and the E3 ligase ITCH in conjunction with the adaptor protein NUMB (Huntzicker et al., 2006; Di Marcotullio et al., 2006). Similar to slmb regulation of the *Drosophila* GLI homolog cubitus interruptus, the mammalian SCF[β-TrCP] is a major regulator of the protein stability and/or proteolytic cleavage of mammalian GLI1 and its paralogs GLI2 and GLI3 (Jiang, 2006; Huntzicker and Oro, 2008). SCF[β-TrCP] is comprised of the bridging protein SKP1, the scaffolding protein CUL1, the substrate-recognizing F-box protein β-TrCP (also known as F-box/WD repeat-containing protein 1A) and the RING finger protein RBX1. This complex catalyzes the transfer of ubiquitin from E2 ligase to the substrate, leading to degradation by the ubiquitin proteasome system (UPS) (Skaar et al., 2013). In cultured human keratinocytes, GLI1
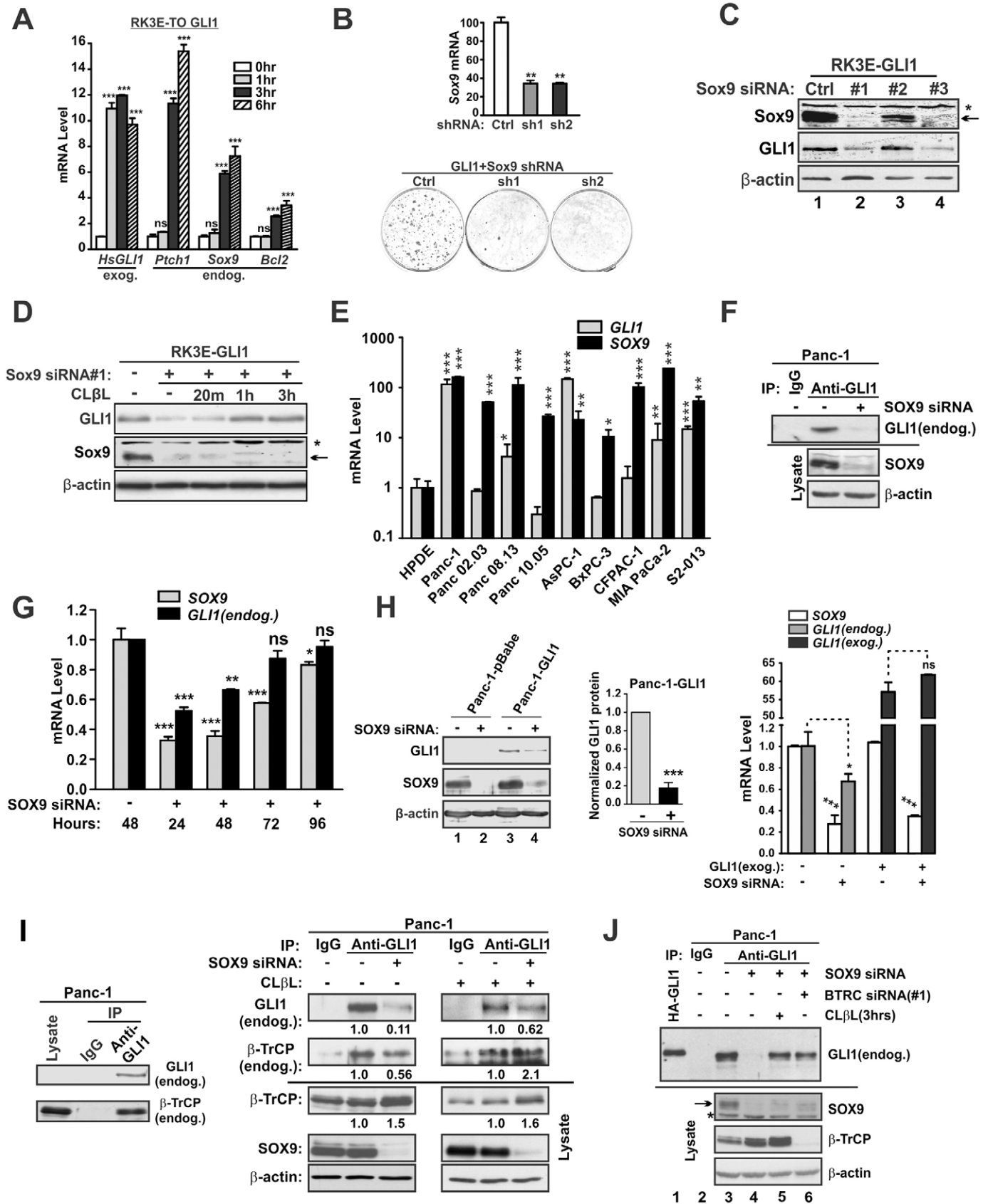
Fig. 1. See next page for legend.

Fig. 1. SOX9 stabilizes GLI1 in the rat RK3E epithelial model and in human PDA cells. (A) Rapid induction of SOX9 by GLI1. RK3E-derived, tet-on (TO) GLI1 cells were induced with tet or with vehicle control, and gene expression was analyzed by qRT-PCR ($n=4$). exog., exogenous; endog., endogenous. (B) Role of SOX9 for GLI1-mediated *in vitro* transformation. Upper panel, *Sox9* shRNA constructs were transfected into RK3E cells. *Sox9* mRNA was analyzed by qRT-PCR following drug selection. Lower panel, GLI1-mediated *in vitro* transformation was assayed in RK3E cells by counting morphologically transformed foci. Dishes are representative of three independent experiments. Background was determined using empty vector and was <1 focus per dish (not shown). (C) Dependence of GLI1 protein expression on SOX9. GLI1-transformed RK3E cells were transfected with the indicated siRNA. Protein expression was analyzed at 48 h post-transfection. The arrow shows the position of SOX9. The asterisk shows a nonspecific band. (D) Proteasome inhibition restores GLI1 in SOX9-deficient cells. GLI1-transformed RK3E cells were transfected with *Sox9* siRNA. Cells were treated with vehicle (DMSO, 1 h) or with proteasome inhibitor (CLβL) for the indicated interval. Cell extracts for protein analysis were prepared at 48 h post-transfection. (E) *SOX9* and *GLI1* were analyzed in human PDA cell lines. mRNA levels were normalized to those of immortalized pancreatic ductal epithelial cells (HPDE). (F) Dependence of GLI1 protein expression on SOX9. Panc-1 cells were treated with control or SOX9 siRNA, and endogenous GLI1 protein levels were determined by immunoprecipitation (IP)-immunoblot analysis. (G) Dependence of *GLI1* mRNA expression on SOX9. Panc-1 cells were treated with siRNA and *SOX9* and *GLI1* mRNA levels were assessed at the indicated post-transfection interval. (H) SOX9 can regulate GLI1 protein levels independently of the mRNA. To circumvent the GLI1 autoregulation of its own transcription, a GLI1 retroviral vector was transduced into Panc-1 cells such that the preponderance of *GLI1* mRNA was transcribed under control of the LTR promoter (Panc-1-GLI1) versus the endogenous *GLI1* promoter (Panc-1-pBabe). The impact of SOX9 deficiency on the GLI1 protein level in Panc-1-GLI1 cells was then analyzed by immunoblotting (left panel). Following normalization to β-actin, the GLI1 protein level in control and SOX9-deficient cells was quantified in three independent assays (middle panel). Similarly, mRNA levels were analyzed by qRT-PCR (right panel). All quantitative data show the mean±s.d. *$P<0.05$; **$P<0.01$; ***$P<0.001$; ns, not significant. Data were analyzed using the unpaired Student's *t*-test (two-tailed) or one-way analysis of variance (ANOVA) followed by Tukey's multiple comparison *ad hoc* post-test. (I) SOX9 regulates the association of GLI1 and β-TrCP. Left panel, endogenous GLI1–β-TrCP interaction in Panc-1 cells was determined by co-IP-immunoblot analysis. Right panel, Panc-1 cells were treated with control siRNA, SOX9 siRNA and/or CLβL as indicated; the endogenous GLI1–β-TrCP interaction was evaluated by co-IP-immunoblot analysis. (J) The role of β-TrCP and the proteasome in the regulation of GLI1 by SOX9. Panc-1 cells were treated as indicated and endogenous protein levels were determined by immunoprecipitation-immunoblot analysis.

stability is dependent upon epidermal growth factor (EGF) signaling through the MEK1/2–ERK1/2 pathway (Kasper et al., 2006). Similarly, in cultured human PDA cells, activated KRAS can stabilize the GLI1 protein through ERK1/2 (also known as MAPK3/1) signaling (Ji et al., 2007). These results suggest a broader role of RAS, MEK1/2 and ERK1/2 in stabilization of GLI1.

GLI1 directly induces the transcription of SOX9, an Sry-like high mobility group (HMG) box transcription factor that plays key roles in sex determination, chondrogenesis and cell differentiation (de Crombrugghe et al., 2001; Kashimada and Koopman, 2010; Barrionuevo and Scherer, 2010). SOX9 responds to Hedgehog–Gli signaling in multiple contexts, including chondrocytes, retinal progenitor cells and developing hair follicles (Tavella et al., 2004; Vidal et al., 2005; McNeill et al., 2012; Eberl et al., 2012). Consistent with these results, the *SOX9* promoter and upstream flanking region contains consensus GLI-binding sites that, when linked to a transcriptional reporter, can be regulated by GLI1 in cultured cells (Bien-Willner et al., 2007; Eberl et al., 2012).

In the developing pancreas, SOX9 is expressed in stem- or progenitor-like cells and is required for normal organogenesis

(Seymour et al., 2007; Lynn et al., 2007). In the adult pancreas, SOX9 is expressed in ductal and centroacinar cells, but is normally expressed at low levels in or absent from acinar cells. Two types of studies have documented a protumorigenic role for SOX9 in PDA. First, xenograft experiments utilizing human PDA cells such as Panc-1 cells indicate that SOX9 promotes the maintenance of tumor-initiating cells (Eberl et al., 2012; Sun et al., 2013). Second, the induction of PanIN lesions in the conditional Kras[G12D] mouse model of PDA involves the early induction of SOX9 in acinar cells, followed by acinar-ductal metaplasia and tumor progression (Kopp et al., 2012). Conditional gene knockout or enforced expression reveals that SOX9 is critical for the occurrence of PanIN lesions. Similarly SOX9 is protumorigenic in other contexts, including colorectal cancer and mammary cancer, promoting the induction of cancer stem cell (CSC) factors such as BMI1 and/or cooperating with mesenchyme-inducing factors such as Snail or Slug (Guo et al., 2012; Matheu et al., 2012).

In the current study, we found that SOX9 is important for efficient *in vitro* transformation by GLI1, a feature attributed to its stabilization of GLI1. Like other SCF[β-TrCP] substrates, GLI1 interacted with the C-terminal WD domain of β-TrCP. SOX9 instead interacted with the N-terminal F-box domain, and yet inhibited the association of GLI1 and β-TrCP. Consistent with a crucial role of the SOX9–β-TrCP interaction for stabilization of GLI1, suppression of β-TrCP in SOX9-deficient PDA cells led to restoration of GLI1 and promoted malignant properties. Because SCF[β-TrCP] can promote the ubiquitylation of functionally diverse proteins, its ultimate role as pro- versus anti-tumorigenic might be context dependent (Frescas and Pagano, 2008; Lau et al., 2012; Shaik et al., 2012; Skaar et al., 2013). Our data suggest that β-TrCP-associated proteins such as SOX9 could be a crucial aspect of this context, capable of suppressing SCF activity against multiple pro-tumorigenic substrates such as GLI1, β-catenin and the anti-apoptotic factor MCL1. These results identify reactivation of latent β-TrCP as a strategy for the disruption of KRAS-mediated protumorigenic signaling.

RESULTS
A role for SOX9 in GLI1-mediated epithelial transformation *in vitro*

RK3E cells, derived from rat kidney cells by immortalization with adenovirus E1A, undergo malignant transformation in response to GLI1 and provide an epithelial context for functional studies (Foster et al., 1999; Li et al., 2006). Utilizing this model, we identified increased levels of *Sox9* mRNA and the corresponding protein as early responses to exogenous human GLI1 (HsGli1, Fig. 1A; supplementary material Fig. S1A). In RK3E cells engineered to induce GLI1 when exposed to tetracycline (RK3E-TO GLI1 cells), the *Sox9* mRNA was induced between 1 and 3 h after drug treatment. Kinetics were similar to those of other well-established GLI1-regulated genes, including *Ptch1* and *Bcl2*. Consistent with a direct interaction, ChIP analyses and luciferase reporter studies identified a candidate enhancer element containing a GLI1 consensus site, located downstream of the rat *Sox9* coding region and ~1.0 kb downstream of exon 3 (supplementary material Fig. S1B–D).

To analyze SOX9, we generated shRNA expression vectors (shSox9-1 and -2) that stably suppressed the *Sox9* mRNA in RK3E cells (Fig. 1B, upper panel). As compared to a non-targeting control (Ctrl), plasmid co-transfection of GLI1 vector with either shRNA construct efficiently inhibited the outgrowth of transformed foci
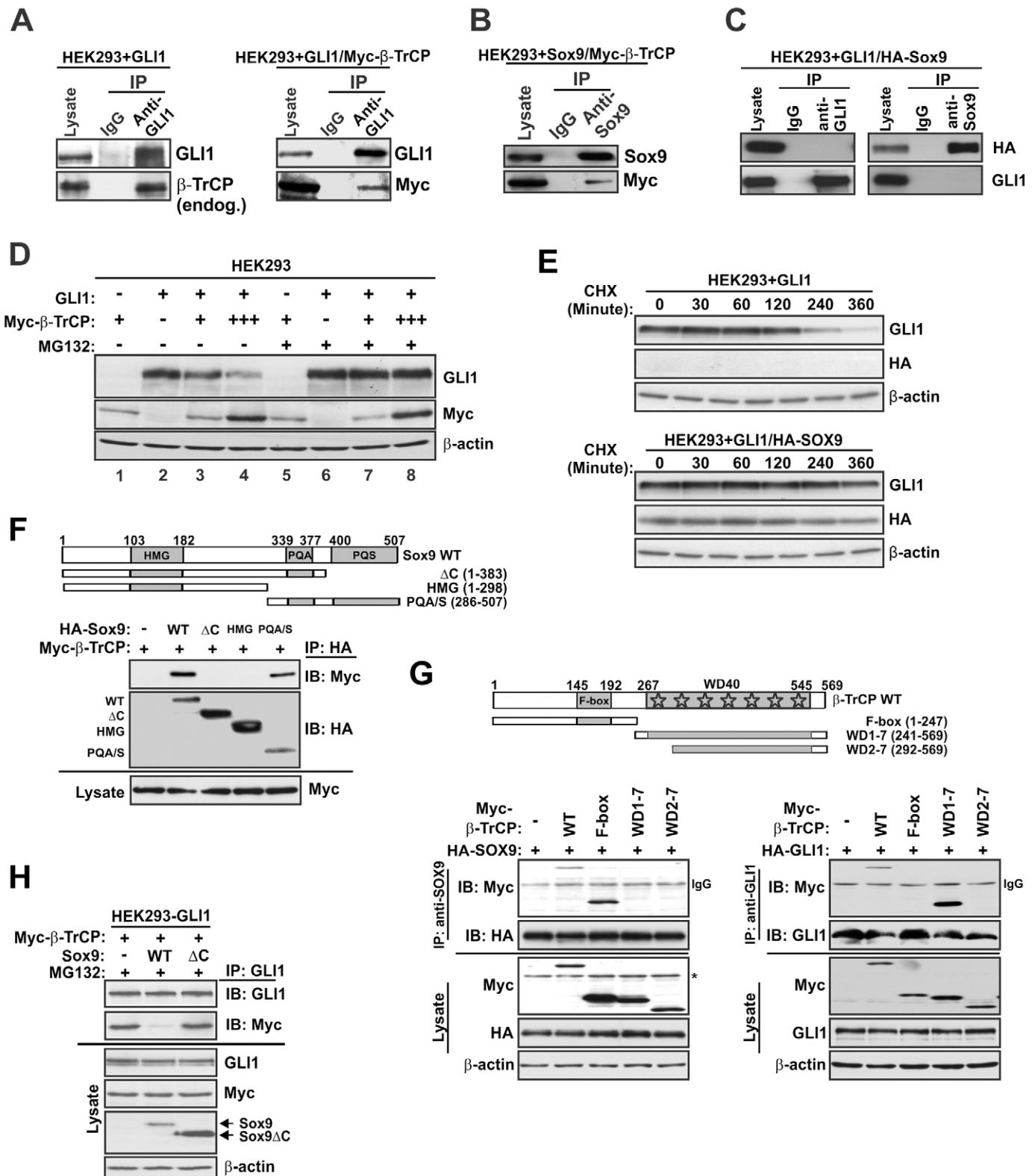
Fig. 2. See next page for legend.

(Fig. 1B, lower panel). By contrast, SOX9 appeared largely dispensable when transformed foci were instead generated using an ERBB2 vector (supplementary material Fig. S1E).

Following small interfering (si)RNA-mediated suppression of SOX9 in GLI1-transformed RK3E cells, we found that GLI1 protein levels were reduced, suggesting a role for SOX9 in the

Fig. 2. SOX9 and GLI1 interact with distinct regions of β-TrCP in a mutually incompatible fashion. Enforced expression studies were performed in HEK293 cells (A–H). (A) Co-IP analysis of GLI1 and β-TrCP. Immunoprecipitated (IP) proteins were analyzed by immunoblot analysis. Lysate lanes represent 5% of the input extract. endog., endogenous. (B) Co-IP analysis of SOX9 and β-TrCP. (C) Co-IP analysis of GLI1 and SOX9. (D) Role of the proteasome in the regulation of GLI1 by β-TrCP. Cells were transfected with the indicated vectors and treated with proteasome inhibitor (MG132) or vehicle (DMSO) for 6 h prior to preparation of cell extracts for immunoblot analysis. (E) Stabilization of GLI1 by SOX9. Cells transfected with the indicated vectors were treated with cycloheximide (CHX) prior to preparation of cell extracts for immunoblot analysis. (F) Co-IP analysis of Myc–β-TrCP with wild-type (WT) or truncated HA–SOX9 constructs. Precipitated proteins were detected by immunoblotting (IB). (G) SOX9 and GLI1 interact with distinct regions of β-TrCP. Co-IP analysis of GLI1 or SOX9 with wild-type or truncated Myc–β-TrCP constructs. Precipitated proteins were detected by immunoblot analysis. The asterisk indicates a nonspecific species. (H) The SOX9 C-terminal region is required for disruption of the GLI1 interaction with β-TrCP. Cells stably transduced with a GLI1 retroviral vector were transfected with the indicated expression vectors. The Myc–β-TrCP plasmid amount was doubled when co-transfected with wild-type SOX9 (middle lane) to achieve similar Myc–β-TrCP protein levels. Cells were treated with MG132 for 3 h before they were harvested for Co-IP analysis. Similar results were obtained in an independent experiment.

maintenance of GLI1 (Fig. 1C, lanes 2 and 4). Treatment with the proteasome inhibitor clasto-lactacystin β-lactone (CLβL) rapidly restored GLI1 protein levels (Fig. 1D). These results identified SOX9 as a transcription factor with a potential role in GLI1 protein stability.

Endogenous SOX9 stabilizes GLI1 in pancreatic cancer cells through regulation of β-TrCP-mediated degradation

Analysis of conditionally deficient mice has shown that SOX9 and GLI1 play crucial roles in PDA development. We analyzed nine PDA tumor cell lines and found that, relative to non-malignant human pancreatic ductal epithelial (HPDE) cells, *SOX9* levels were markedly upregulated (10- to 240-fold), and most lines likewise expressed increased levels of *GLI1* (Fig. 1E).

To examine a role for endogenous SOX9, we utilized transient or inducible siRNAs that target two distinct sequences (supplementary material Fig. S2A). To detect endogenous GLI1, a low abundance factor, we utilized immunoprecipitation and immunoblot analysis. Using this assay, either of two different GLI1 antibodies identified a protein of 150 kDa (supplementary material Fig. S2B and data not shown). Repression of SOX9 in PDA cells resulted in the reduction of endogenous GLI1 protein levels (Fig. 1F), and mRNA analysis revealed synchronous loss of both *SOX9* and *GLI1* signals after siRNA transfection (Fig. 1G).

To analyze how SOX9 regulates GLI1, we engineered PDA cells that independently regulate the GLI1 mRNA and protein, through introduction of a *GLI1* transgene under the control of a retroviral promoter (Panc-1-GLI1). In these cells, the exogenous GLI1 protein was reduced following SOX9 knockdown (Fig. 1H, lanes 3, 4). Three independent experiments indicated loss of 82% of the GLI1 (Fig. 1H, middle panel). By contrast, the *GLI1* transgene-derived mRNA levels were not dependent upon SOX9 (Fig. 1H, right panel). In vector control cells, the suppression of SOX9 repressed the endogenous *GLI1* mRNA. These results indicate that loss of *GLI1* mRNA following SOX9 suppression is due to destabilization of the GLI1 protein and its autoregulation of *GLI1* transcription.

Interaction of endogenous GLI1 and β-TrCP proteins was readily detected in human PDA cells (Fig. 1I, left panel). In the

absence or presence of proteasome inhibitor the suppression of endogenous SOX9 increased the ratio of β-TrCP:GLI1 in immunoprecipitates (Fig. 1I, right panel). Similar to results observed following treatment with proteasome inhibitor, GLI1 expression was rescued by suppression of β-TrCP (Fig. 1J, lanes 5, 6). Similar results were obtained using transient SOX9 siRNA or the TO conditional approach in either Panc-1 or AsPC-1 cells (supplementary material Fig. S2C).

SOX9 disrupts the interaction of GLI1 with β-TrCP

SOX9 was previously shown by co-immunoprecipitation (co-IP) and colocalization studies to associate with β-TrCP, likely through the SOX9 C-terminus, as deletion of this region abrogated binding (Topol et al., 2009). To investigate whether the association of SOX9 with β-TrCP can modulate the targeting of GLI1 for ubiquitylation, we utilized HEK293 cells that contain very low levels of endogenous SOX9. When expressed by transient transfection, GLI1 was found to associate with both endogenous and exogenous β-TrCP (Fig. 2A). Similar to previous reports (Topol et al., 2009), the SOX9–β-TrCP interaction was readily detected (Fig. 2B). However, in multiple experiments we were unable to observe any association of GLI1 and SOX9 (Fig. 2C). Negative results were obtained for co-IP of endogenous proteins in Panc-1 cells as well as overexpressed proteins in HEK293, using both forward and reverse co-IP strategies. These results suggested that SOX9 might not regulate GLI1 through a direct interaction but rather could regulate its association with the E3 ligase component β-TrCP.

Consistent with the established role of β-TrCP in GLI1 regulation, GLI1 levels were suppressed by transient delivery of exogenous β-TrCP, and restored by addition of proteasome inhibitor (Fig. 2D). In contrast to GLI1, there was no suppression of SOX9 levels in response to β-TrCP (supplementary material Fig. S2D). These results suggest that exogenous SOX9 might prevent the binding of GLI1 to its E3 ligase and the subsequent ubiquitylation (Huntzicker et al., 2006). Indeed, an assay of GLI1 stability using the protein synthesis inhibitor cycloheximide (CHX) showed that SOX9 could extend the half-life of this protein (Fig. 2E).

SOX9 contains three conserved domains – HMG, PQA and PQS (Fig. 2F). The HMG box mediates DNA binding, whereas PQA and PQS promote transactivation. Deletion analysis indicated that the transactivation region (fragment PQA/S) is sufficient to interact with β-TrCP, and with comparable efficiency to that of wild-type SOX9 (Fig. 2F). As reported previously (Topol et al., 2009), deletions within the transactivation domain (ΔC or HMG) abrogated the interaction.

The WD40 repeats of β-TrCP mediate substrate binding, and the first WD40 repeat plays a crucial role in substrate recognition (Skaar et al., 2013). By contrast, the F-box region mediates interaction with SKP1. Consistent with lack of a suppressive effect of β-TrCP on SOX9 (supplementary material Fig. S2D), and unlike SCF$^{\beta-TrCP}$ substrates or pseudosubstrates (Davis et al., 2002), deletion analysis indicated that SOX9 associated with the F-box region of β-TrCP (Fig. 2G, left panel). As expected for a substrate, GLI1 interacted with the WD40 repeats of β-TrCP (fragment WD1-7), and deletion of the first WD40 repeat (fragment WD2-7) abrogated this interaction (Fig. 2G, right panel). Although they interacted with distinct β-TrCP domains, co-IP of GLI1 and β-TrCP was nevertheless markedly suppressed in the presence of SOX9 (Fig. 2H, lane 2). By contrast, the co-expression of SOX9ΔC, deficient for β-TrCP binding, had little
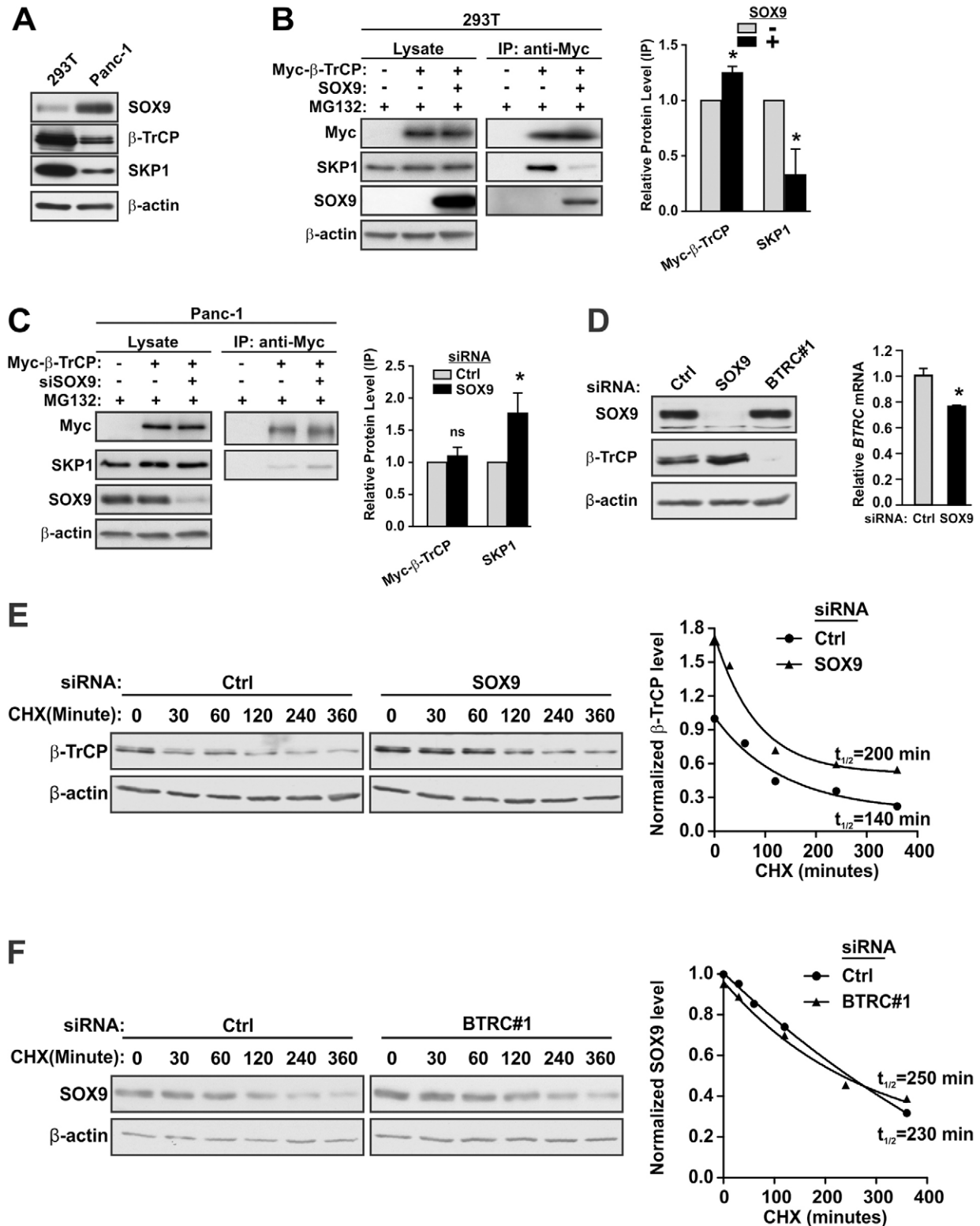
Fig. 3. See next page for legend.

effect (Fig. 2H, lane 3). Unlike for β-TrCP, using reciprocal co-IPs, we observed no interaction of SOX9 with other F-box proteins, including FBXW7 and SKP2 (supplementary material Fig. S2E; data not shown).

SOX9 interferes with SKP1 binding and facilitates β-TrCP turnover in pancreatic cancer cells

As SOX9 interacted with F-box region of β-TrCP, we asked whether this association would interfere with β-TrCP–SKP1

Fig. 3. SOX9 disrupts the β-TrCP–SKP1 association and destabilizes β-TrCP in PDA cells. (A) Relative levels of SOX9, β-TrCP and SKP1 protein in HEK293T and Panc-1 cells. (B) The effect of exogenous SOX9 on the association of SKP1 and β-TrCP. 293T cells were transfected with the indicated expression vectors. Myc–β-TrCP plasmid amounts were doubled when co-transfected with wild-type SOX9 to achieve similar levels of Myc–β-TrCP protein expression. Cells were treated with MG132 for 3 h before they were harvested for co-IP analysis. The results of three independent experiments are indicated. IP, immunoprecipitation. (C) Effect of endogenous SOX9 on the association of SKP1 and β-TrCP. Panc-1 cells were transfected with the indicated expression vectors and siRNAs. Cells were treated with MG132 for 3 h before being harvested for co-IP analysis. The results of three independent experiments are indicated. (D) The effect of SOX9 on expression of β-TrCP. Panc-1 cells were treated with the indicated siRNA and then analyzed by immunoblot analysis (left panel) or by qRT-PCR (right panel). Quantitative data in B–D show the mean±s.d. *$P<0.05$; ns, not significant. Data were analyzed using the unpaired Student's *t*-test (two-tailed). (E,F) Analyses of protein stability. Panc-1 cells were transfected with the indicated siRNA and then treated with cycloheximide (CHX) for the indicated interval prior to the preparation of extracts for immunoblot analysis at 48 h post-transfection. The scanned images were quantified using NIH ImageJ and normalized to β-actin. Rate constants and protein half-lives were determined using the first order rate law.

binding. 293T cells contain much lower levels of endogenous SOX9 compared with Panc-1 cells (Fig. 3A). In 293T cells, the binding of Myc–β-TrCP to endogenous SKP1 was suppressed by a mean of 67% in the presence of exogenous SOX9 (Fig. 3B; three independent experiments). Conversely, the binding of Myc–β-TrCP to endogenous SKP1 was increased by a mean of 76% following SOX9 knockdown in Panc-1 cells (Fig. 3C; three independent experiments). These results identify interference with the β-TrCP–SKP1 association as a mechanism by which SOX9 can stabilize GLI1.

In PDA cells, SOX9 suppression resulted in consistent increases in β-TrCP protein levels relative to the mRNA (Fig. 3D; see also the lysate panels in Fig. 1I, right panel; Fig. 1J; supplementary material Fig. S2C). Coexpression of SOX9 with β-TrCP in HEK293 or Panc-1 cells promoted β-TrCP degradation (supplementary material Fig. S2D; data not shown). We therefore determined the half-life of SOX9 and β-TrCP proteins in control PDA cells and in cells deficient in SOX9 or β-TrCP. Knockdown of SOX9 increased the steady-state abundance of β-TrCP and extended its half-life from 140 to 200 minutes (Fig. 3E). By contrast, β-TrCP suppression did not significantly alter the expression or stability of SOX9, which had a half-life of ~230 minutes in control cells (Fig. 3F). These results identify distinct inhibitory effects of SOX9 on SCF$^{β-TrCP}$.

SOX9 tethers β-TrCP within the nucleus and selectively protects nuclear GLI1 from degradation
Both SOX9 and β-TrCP are primarily localized in the cell nucleus (Davis et al., 2002; Vidal et al., 2005; Wang et al., 2007; Topol et al., 2009). We analyzed the effect of endogenous SOX9 on the localization of transiently expressed Myc–β-TrCP in PDA cells. As previously shown for primary chondrocytes (Topol et al., 2009), SOX9 appeared to efficiently tether β-TrCP in this compartment (Fig. 4A). In SOX9-deficient PDA cells, the β-TrCP was instead dispersed throughout the cell such that the nuclear staining was reduced and cytoplasmic staining was increased.

Exogenous GLI1 was detected in both the nucleus and the cytoplasm (Fig. 4B, upper row). In SOX9-deficient cells, GLI1 was preferentially lost from the cell nucleus, but cytoplasmic

staining was preserved (Fig. 4B, middle row). Consistent with a UPS role in the suppression of nuclear GLI1, treatment of cells with CLβL restored nuclear staining (Fig. 4B, lower row). This immunostaining data appeared to be consistent with the partial suppression of exogenous GLI1 observed by immunoblot analysis (Fig. 1H). The more complete suppression observed for endogenous GLI1 (Fig. 1F,I,J; supplementary material Fig. S2C) remains unexplained, but could reflect its preferential nuclear localization relative to that of the overexpressed protein. These results support a role for SOX9 in tethering β-TrCP within the nucleus of PDA cells. Selective loss of nuclear GLI1 upon suppression of SOX9 indicates that nuclear SCF$^{β-TrCP}$ activity is increased despite the dispersal of β-TrCP throughout the cell. These results suggest that the apparent β-TrCP concentration can be discordant with its activity when SOX9 is present.

### SOX9 promotes the malignant properties of PDA cells in a fashion dependent upon β-TrCP and GLI1
Both SOX9 and GLI1 appear to be crucial for tumorigenesis in PDA (Rajurkar et al., 2012; Kopp et al., 2012; Mills et al., 2013). Although SOX9-deficient Panc-1 cells fail to form tumors in a mouse xenograft assay, potential links to GLI1 function remain unexplored (Eberl et al., 2012). For SOX9-deficient and control PDA cells we analyzed several *in vitro* correlates of the malignant phenotype, including proliferation, anchorage independence and survival. SOX9-deficient Panc-1 cells proliferated in two-dimensional (2D) culture similarly to control cells (Fig. 5A), but were unable to efficiently form colonies in soft agar over a period of 2 weeks (Fig. 5B). Other PDA cell lines, AsPC-1 and MiaPaCa-2, responded similarly. When cells were suspended in low attachment plates for 24 or 48 h (anoikis assay), deficiency in SOX9 resulted in a marked reduction in the overall viable cell number and the proportion of viable cells (Fig. 5C). These results confirm that SOX9 deficiency can abrogate the malignant properties of PDA cells.

We used the anoikis assay to determine whether deficiency of SCF$^{β-TrCP}$ substrates such as GLI1 might be responsible for the loss of malignant properties. We restored GLI1 expression in SOX9-deficient cells using β-TrCP siRNAs (Fig. 5D; supplementary material Fig. S3A). The cell death phenotype of SOX9-deficient PDA cells was attenuated by co-suppression of β-TrCP in both Panc-1 and AsPC-1 cells. Consistent with a functional role for GLI1 as a mediator of the increased cell survival following β-TrCP suppression, co-suppression of GLI1 promoted cell death (Fig. 5E).

SOX9 promotes the CSC-like properties of PDA cells in a β-TrCP-dependent fashion
CSCs are an aggressively malignant subset of tumor cells (Clevers, 2011). In PDA, both SOX9 and GLI1 are important for the maintenance of this subpopulation (Eberl et al., 2012; Tang et al., 2012; Sun et al., 2013; Li et al., 2013). To determine whether there is phenotypic overlap following modulation of SOX9 or GLI1, we enriched for CSCs using spheroid formation or dye efflux assays (i.e. side population cells) (Bhagwandin and Shay, 2009) (Fig. 6A). In addition to GLI or GLI-regulated factors (*GLI1*, *GLI2*, *SOX9*, *SNAI1*), these subpopulations had increased levels of pancreatic CSC markers (*CD24*, *CD44*, *ESA*, *CD133* and *CXCR4*) as well as factors important for the generation of induced pluripotent stem cells (*OCT4* and *KLF4*) (Takahashi and Yamanaka, 2006; Li et al., 2007; Hermann et al., 2007) (Fig. 6B). Consistent with a role for GLI1 in the phenotype
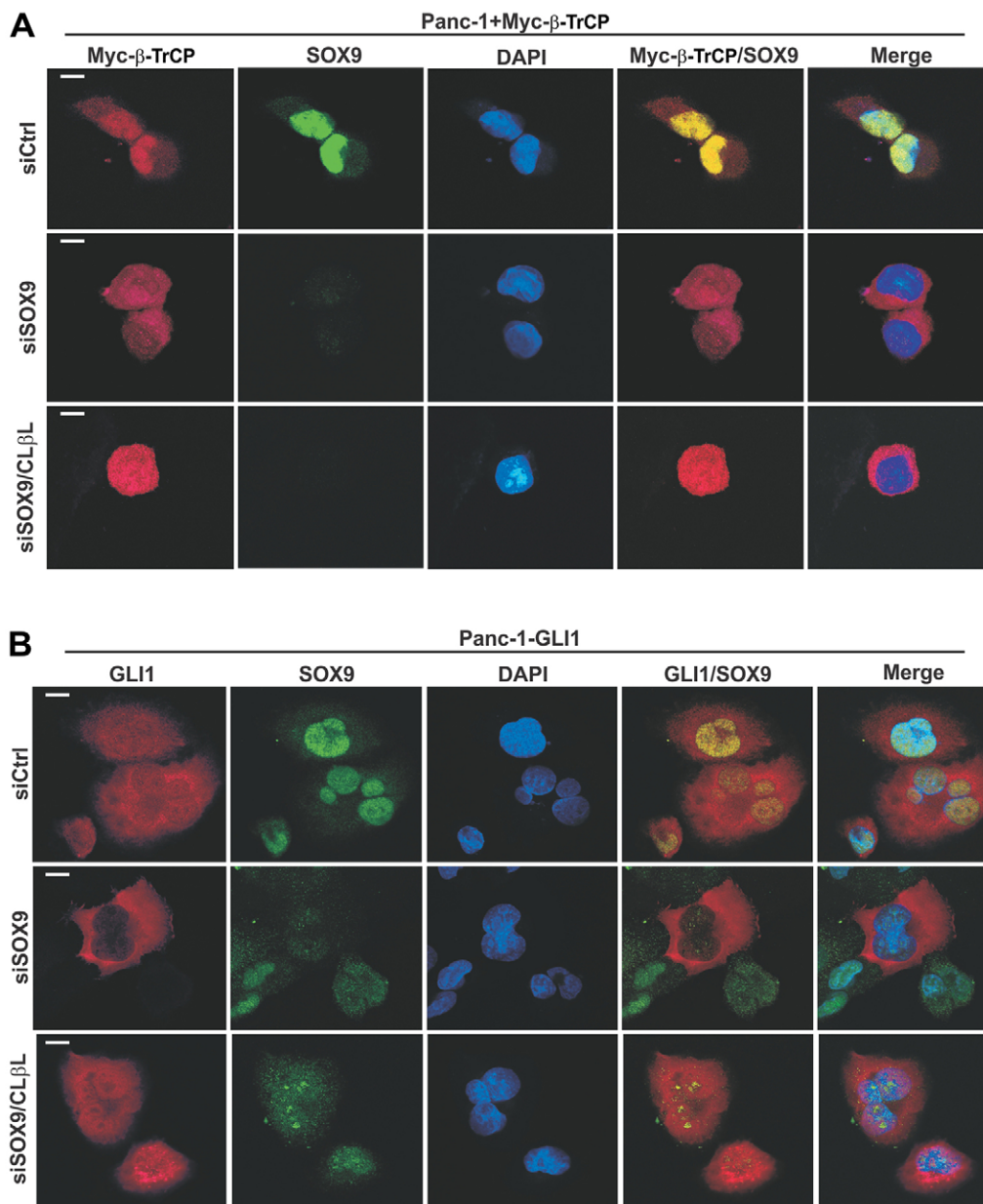
Fig. 4. SOX9 tethers β-TrCP within the nuclei of PDA cells and protects nuclear GLI1 from degradation. (A) Panc-1 cells were transfected with exogenous Myc-tagged β-TrCP together with the indicated siRNA. (B) Panc-1 cells were infected with the lentiviral GLI1 vector and then with the indicated siRNA. Cells were treated with CLβL or vehicle (DMSO) for the final 3 h prior to fixation. Cells were fixed and processed for indirect immunofluorescence analysis at 48 h post-transfection. Scale bars: 10 µm.

of SOX9-deficient cells, suppression of either gene product in 2D cultures of PDA cells reduced the expression of CSC markers, resulting in very similar profiles (Fig. 6C).

We next examined whether β-TrCP suppression could rescue the CSC phenotype in SOX9-deficient cells. Stable suppression of SOX9 reduced spheroid formation by 75% (Fig. 6D). Consistent with this result, SOX9 suppression in 2D-cultured PDA cells also reduced the abundance of side population cells (Fig. 6E; supplementary material Fig. S3B). Without SOX9 suppression, transient suppression of β-TrCP had little effect on spheroid growth (Fig. 6F, left panel). However, in SOX9-deficient cells, siβ-TrCP partially rescued spheroid formation (Fig. 6F; supplementary material Fig. S3C). The remarkably similar expression profile in SOX9- and GLI1-deficient tumor cells, and restoration of spheroid formation by siβ-TrCP support a role for the suppression of SCF$^{β\text{-}TrCP}$ activity as a mechanism by which SOX9 can promote GLI1 expression and the CSC-like phenotype.

SOX9 is increased whereas β-TrCP is decreased in primary human PDA

The above data indicate that SOX9 functions in cultured PDA cells to antagonize β-TrCP expression and its activity towards GLI1. We utilized Oncomine microarray data (Compendia Bioscience) to analyze SOX9 and β-TrCP expression in primary human PDA specimens (Rhodes et al., 2004). Four studies each detected increased levels of PDA signature genes, typified by *SFN* (also known as *14-3-3σ*), in PDA tumor tissue relative to morphologically normal tissue (Logsdon et al., 2003; Iacobuzio-Donahue et al., 2003; Segara et al., 2005; Badea et al., 2008; Pei et al., 2009) (supplementary material Table S1 and Fig. S4). In these studies, *SOX9* mRNA expression was upregulated (1.00- to 1.87-fold), whereas transcripts encoding β-TrCP (*BTRC*) were consistently repressed (1.12- to 1.25-fold). This increase in *SOX9* and decrease in *BTRC* expression might contribute to the upregulation of GLI1 in PDA (Thayer et al., 2003; Feldmann et al., 2007; Nolan-Stevaux et al., 2009).
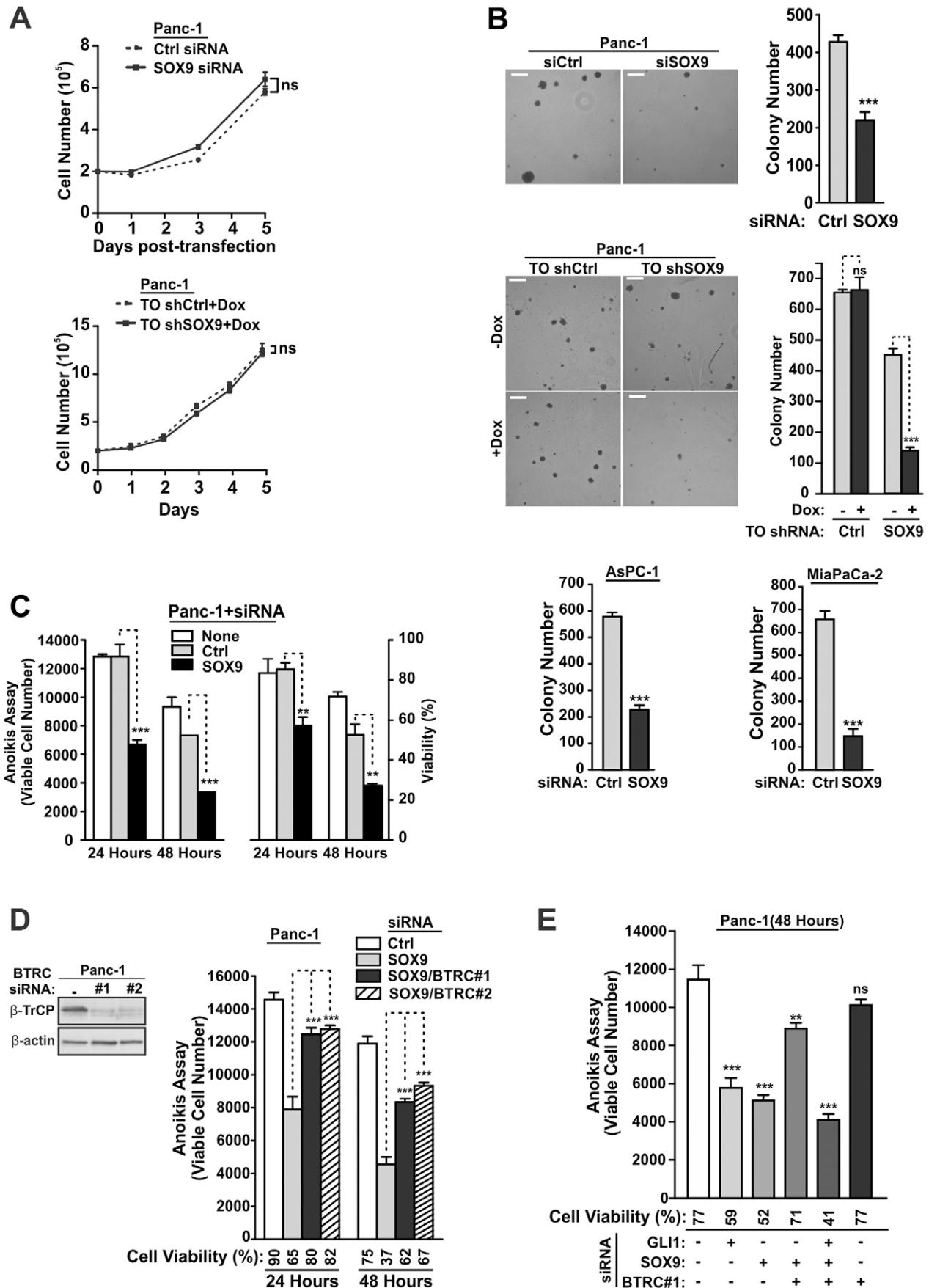
Fig. 5. See next page for legend.

Fig. 5. In a GLI1-dependent fashion, β-TrCP suppression rescues malignant properties in SOX9-deficient PDA cells. (A) Panc-1 cell growth in 2D culture was analyzed following transfection of SOX9 or control siRNAs (upper panel). Alternatively, Panc-1-TO shRNA cells were treated with Dox (lower panel). (B) Analysis of anchorage-independent growth regulation by SOX9. A soft agar assay was performed using Panc-1 cells (n=3). Similar results are shown for AsPC-1 and MiaPaCa-2 cell lines (lower panels). Scale bars: 400 µm. (C) Analysis of anoikis regulation by SOX9. The anoikis assay was performed using Panc-1 cells. The number of surviving cells (left y-axis) and the percentages of viable cells (right y-axis) are indicated for each timepoint (n=3). (D,E) Role of β-TrCP in the phenotype of SOX9-deficient cells. Following siRNA transfection, anoikis assays were performed in Panc-1 cells. All quantitative data show the mean±s.d. **P<0.01; ***P<0.001; ns, not significant. Growth curves were analyzed using non-linear regression curve fitting. Other quantitative data were analyzed using the unpaired Student's t-test (two-tailed) or one-way ANOVA followed by Tukey's multiple comparison $ad\ hoc$ post-test.

SOX9 stabilizes other β-TrCP-regulated proteins

If SOX9 selectively stabilizes nuclear GLI1 by antagonizing β-TrCP activity in this compartment, then other substrates might be similarly affected, potentially with more subtle effects for cytoplasmic substrates. Consistent with their known regulation by SCF$^{β\text{-}TrCP}$, β-catenin, Snail and MCL1 protein levels were each reduced by similar amounts to 50% of control levels following SOX9 knockdown in PDA cells, and CLβL treatment restored the levels (Fig. 7A) (Polakis, 1999; Zhou et al., 2004; Ding et al., 2007). For β-catenin, consistent results were obtained with a transcriptional reporter assay (Fig. 7B) and immunofluorescence analysis (Fig. 7C). Cells transfected with SOX9 siRNA had similar to 50% reduction in the expression of both nuclear and cytoplasmic β-catenin (Fig. 7C; supplementary material Fig. S3D). These data are consistent with a predominant role of SOX9 in the nuclear tethering and suppression of SCF$^{β\text{-}TrCP}$ activity through protein–protein interaction, with more subtle effects in the cytoplasm attributed to alterations in β-TrCP concentration (Fig. 4A). Fig. 7D presents a model summarizing the observed effects of SOX9 on β-TrCP and nuclear GLI1.

DISCUSSION

SOX9 is crucial for diverse developmental processes including sex determination, chondrogenesis and pancreatogenesis (de Crombrugghe et al., 2001; Kashimada and Koopman, 2010; Barrionuevo and Scherer, 2010). For cancers of the prostate, colorectum, pancreas and breast, SOX9 plays important roles in carcinoma cell malignant properties (Vidal et al., 2005; Wang et al., 2008; Eberl et al., 2012; Kopp et al., 2012; Guo et al., 2012; Matheu et al., 2012; Sun et al., 2013). In chondrocytes, SOX9 induces the transcription of genes such as COL2A1, COL11A2 and aggrecan (de Crombrugghe et al., 2001; Oh et al., 2010; Pritchett et al., 2011). Although SOX9-responsive genes were analyzed in several contexts, the mechanisms by which SOX9 promotes malignant properties remain poorly understood, and the relative importance of transcriptional signaling versus other biochemical activities is unclear (Lynn et al., 2007; Bhandari et al., 2012; Guo et al., 2012).

In rat RK3E epithelial cells, we identified *Sox9* as an early transcriptional response to GLI1, and linked this regulation to a downstream *Sox9* enhancer element using ChIP and transcriptional reporter studies. These data are consistent with previous reports indicating regulation of mouse or human *SOX9* by Hedgehog and/or GLI1 (Tavella et al., 2004; Vidal et al., 2005; McNeill et al., 2012; Eberl et al., 2012). In analyzing GLI1-transformed cells we were surprised to observe a pronounced loss

of GLI1 protein stability upon suppression of SOX9, attributed to UPS-mediated degradation. This effect was conserved in human PDA cells and indicated a consistent role for SOX9 in stabilization of GLI1.

In a previous study focused upon chondrocytes, SOX9 was found to associate with β-TrCP and to promote β-TrCP nuclear localization and the degradation of nuclear β-catenin (Topol et al., 2009). In the current study focused upon PDA, we found that SOX9 likewise functions as a nuclear tether for β-TrCP, but few other aspects of the chondrocyte study appeared to extend to the PDA context. We instead obtained extensive data supporting a potent inhibitory role for SOX9 on β-TrCP activity in the nucleus. Suppression of β-TrCP in SOX9-deficient cells restored GLI1 levels and promoted phenotypes attributed to SOX9 or GLI1. Supporting the identification of GLI1 as a major factor in the altered phenotype of SOX9-deficient cells, the CSC marker profile of SOX9- or GLI1-deficient PDA cells was remarkably similar.

Consistent with an inhibitory effect on SCF$^{β\text{-}TrCP}$, SOX9 interacted through its PQA/S region with the F-box domain of β-TrCP and suppressed the association of β-TrCP with either endogenous or exogenous SKP1. Typical of other substrates, GLI1 associated with the WD domain. Co-IP assays indicated that GLI1 and SOX9 are mutually incompatible for β-TrCP association. Indeed, in SOX9-deficient PDA cells, the association of GLI1 with β-TrCP was increased by several fold. It is unclear why SOX9 association with the F-box region would prevent GLI1 from binding to the WD domain. Possibilities include steric hindrance, a conformational shift or that SOX9 could facilitate the binding of other nuclear proteins such as hnRNP-U, a WD domain-binding pseudosubstrate, and thereby prevent the association of β-TrCP with GLI1 (Davis et al., 2002).

An additional effect that strongly supported the inhibition of SCF$^{β\text{-}TrCP}$ by SOX9 was the destabilization of β-TrCP. Whether this instability results from the reduced association with SKP1, from tethering within the nuclear compartment and/or from some other effect of SOX9 or yet another associated factor is currently unclear.

In SOX9-deficient PDA cells, β-TrCP was more widely distributed throughout the cell, with reduced nuclear staining and approximately a twofold increase in cytoplasmic staining compared with that of control cells. This redistribution appeared to impact on not only nuclear GLI1 but also cytoplasmic proteins such as the SCF$^{β\text{-}TrCP}$ substrate β-catenin. While nuclear GLI1 was markedly destabilized, the cytoplasmic substrate β-catenin was suppressed by ~50%. Similar effects were observed for two other well-established substrates of SCF$^{β\text{-}TrCP}$, Snail and MCL1. These results indicate a broad role for SOX9 in the regulation of protein stability.

In SOX9-deficient PDA cells, the effects of untethered β-TrCP were quite distinct for nuclear and cytoplasmic GLI1. These results appear to indicate that nuclear GLI1 is selectively targeted by β-TrCP, although the mechanism(s) responsible for this selectivity is unclear. The results are overall consistent with identification of the *Drosophila* homolog as a short-lived nuclear transcriptional activator in response to Hedgehog signaling (Ohlmeyer and Kalderon, 1998). We conclude that when SOX9 is present, the β-TrCP nuclear staining intensity can be discordant with nuclear SCF$^{β\text{-}TrCP}$ activity.

Mouse model data have established clear roles for GLI1 and SOX9 in the malignant progression of PDA (Pasca di Magliano et al., 2006; Ji et al., 2007; Feldmann et al., 2007; Nolan-Stevaux
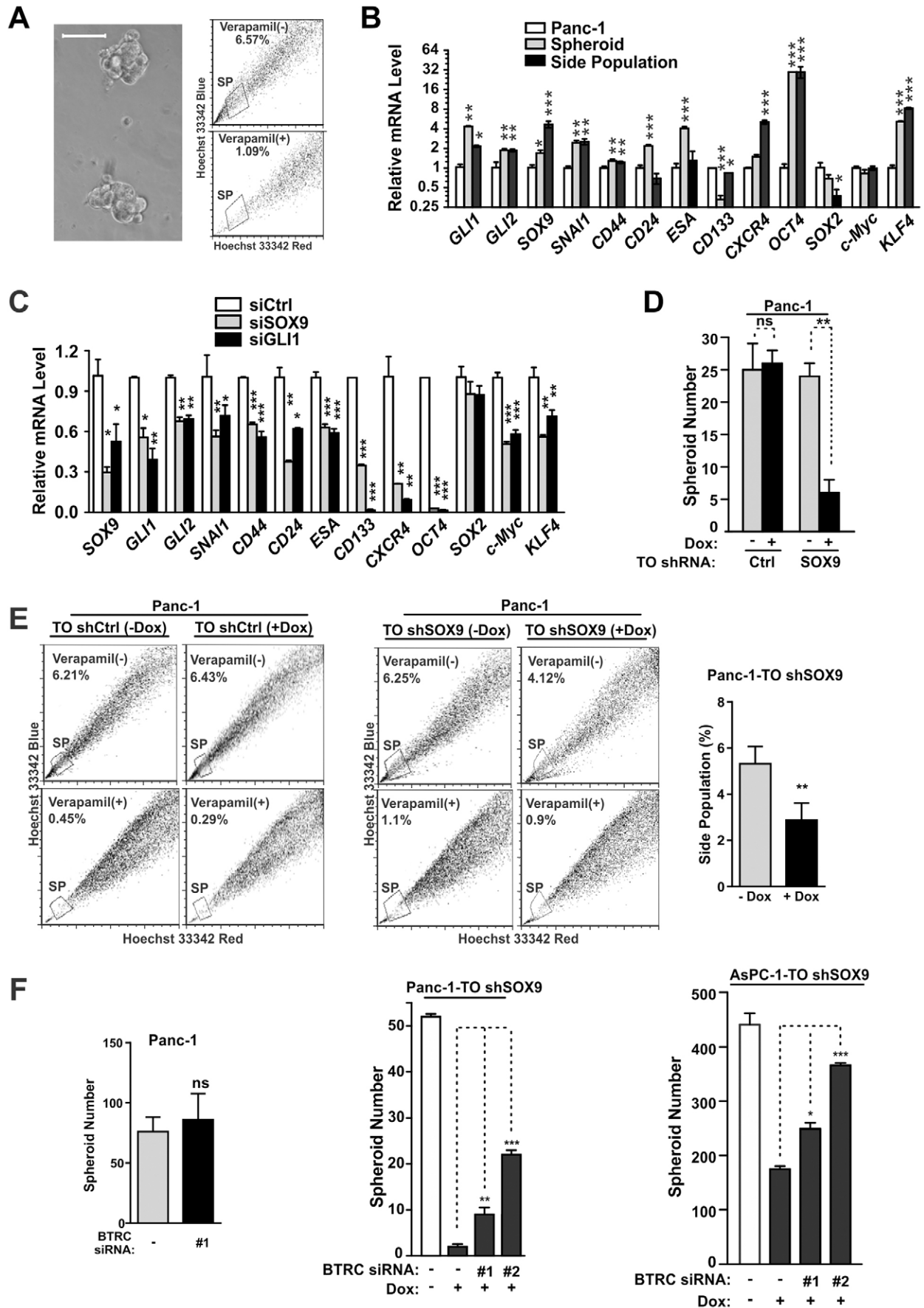
Fig. 6. See next page for legend.

Fig. 6. β-TrCP suppression rescues CSC properties in SOX9-deficient PDA cells. (A) Panc-1 cells form spheroids when suspended in stem cell growth medium (left panel). Scale bar: 200 µm. Side population (SP) Panc-1 cells were identified by verapamil-sensitive dye efflux (right panel). (B) Expression profiling of spheroid cells and side population cells. (C) Roles of SOX9 and GLI1 in the regulation of CSC markers. The expression of putative CSC markers was determined in Panc-1 cells treated with the indicated siRNA. (D) Spheroid formation assay of Panc-1-TO shRNA cells (n=3). (E) Side population analysis of PDA cells. Cells were treated with Dox or vehicle for 5 days and then stained with Hoechst 33342. The results of three independent experiments are presented (right panel). (F) Role of β-TrCP in the growth of tumor spheroids. siβ-TrCP had little effect on its own in parental Panc-1 cells (left panel). The effect of siβ-TrCP was then analyzed in the context of SOX9-deficient PDA cells (middle and right panels). All quantitative data show the mean±s.d. *P<0.05; ** P<0.01; *** P<0.001; ns, not significant.
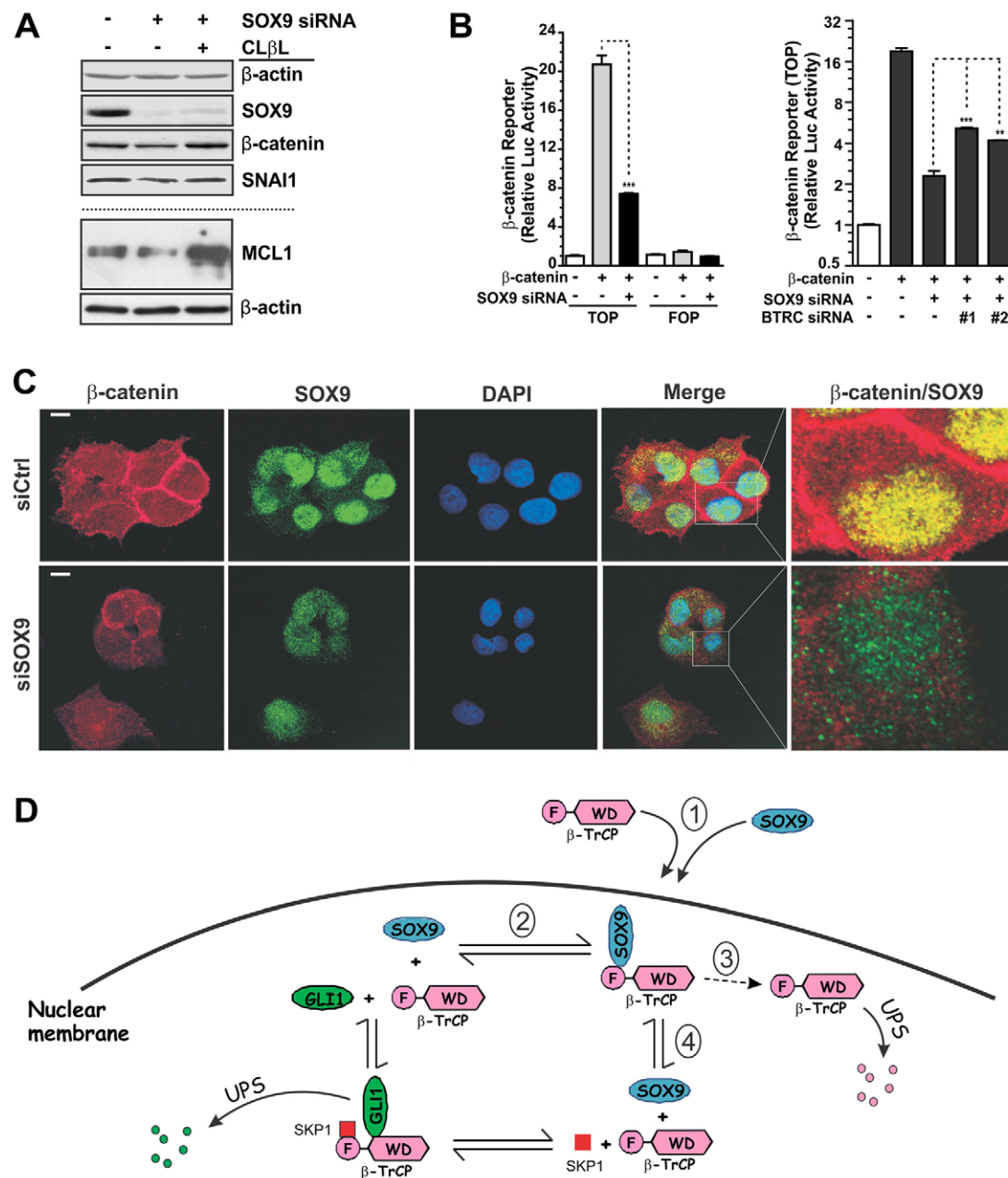
et al., 2009; Rajurkar et al., 2012; Eberl et al., 2012; Kopp et al., 2012; Mills et al., 2013). Interestingly, both SOX9 transcript levels and GLI1 protein stability appear to be crucially dependent upon upstream signaling by RAS–MEK–ERK, but it remains unclear how either factor is regulated by this signaling (Murakami et al., 2000; Kasper et al., 2006; Ji et al., 2007; Eberl et al., 2012). Whereas a *Sox9* transgene directed to the pancreatic acinar cells is sufficient on its own to initiate early PanIn lesions in mice, a *GLI* transgene does not induce these lesions, suggesting that GLI is the more dependent factor (Pasca di Magliano et al., 2006; Kopp et al., 2012). These considerations suggest that KRAS might stabilize GLI1 by signaling through SOX9. Alternatively, it is possible that activated KRAS could more directly regulate GLI1 or both transcription factors in parallel. Blockade of this KRAS signaling in tumor cells, a current focus of research, has the potential to suppress SOX9

Fig. 7. SOX9 stabilizes β-catenin in Panc-1 cells. (A) Regulation of diverse SCF$^{β\text{-TrCP}}$ substrates by SOX9. Panc-1 cells were treated with the indicated siRNA and protein expression was analyzed by immunoblotting. (B) Regulation of β-catenin activity by SOX9 and β-TrCP. Panc-1 cells were transfected with the indicated siRNA and TCF4-dependent transcriptional activity was determined by using a luciferase reporter assay. Data show the mean±s.d. **P<0.01; ***P<0.001. (C) Regulation of β-catenin protein expression by SOX9. Panc-1 cells were treated with the indicated siRNA and then analyzed by indirect immunofluorescence analysis. Scale bars: 10 µm. Quantification of β-catenin is shown in supplementary material Fig. S3D. (D) A model depicting the effects of SOX9 on β-TrCP in PDA cells, including nuclear tethering (1), disruption of its association with GLI1 (2), promotion of UPS-mediated turnover (3) and disruption of its association with SKP1 (4).

and to activate β-TrCP-mediated degradation of multiple oncoproteins.

MATERIALS AND METHODS

Expression vectors and plasmid transfection

pcDNA4/TO-HA-GLI1 was described previously (Li et al., 2006). Retroviral vectors were made by inserting the HAGLI1 cassette of pcDNA4/TO-HA-GLI1 into pB-puro and pLUT7. pLUT7 was provided by Alexey Ivanov (West Virginia University School of Medicine). The human SOX9 expression vector, HA3 SOX9 pcDNA3.1, was a gift from Benoit de Crombrugghe (MD Anderson Cancer Center).

Mouse β-TrCP1 vector containing a 3×Myc epitope tag at the N-terminus (Wan et al., 2004), a gift from Xu Cao (Johns Hopkins University School of Medicine), was used to generate truncated constructs by PCR. All cloned PCR products were verified by sequencing. A human ubiquitin vector, Myc-Ub, was provided by Alexey Ivanov. pcDNA3-β-catenin (Addgene 16828) was a gift from Eric Fearon (University of Michigan Medical School) (Kolligs et al., 1999). pCMV-Myc CDC4 WT* was a gift from Bert Vogelstein (Johns Hopkins University School of Medicine; FBXW7, Addgene plasmid 16652). pcDNA3-myc-Skp2 was a gift from Yue Xiong (University of North Carolina at Chapel Hill; Addgene plasmid 19947).

pTRIPZ-TOshSOX9 lentivector was generated by transfer of the shRNAmir cassette from pGIPZ (V3LHS_396212, Thermo Scientific). Non-targeting TRIPZ lentiviral shRNAmir RHS4743 served as a control. shRNA vectors targeting rat *Sox9* (RnSox9) were constructed in pSilencer 2.1-U6 neo as described previously (Li et al., 2006). shRNA target sequences are listed in supplementary material Table S2.

Retroviral transduction was performed as described previously (Foster et al., 1999). Transient transfections were performed as described previously (Lin et al., 2011) using Lipofectamine 2000 Transfection Reagent (Life Technologies) for Panc-1 cells and TransIT-LT1 Reagent (Mirus) for other cells.

Isolation of rat *Sox9* cDNA and generation of *Sox9* expression vectors

PCR was used to synthesize cDNA fragments containing the RnSox9 5′UTR and protein coding regions. The sequence has been deposited with the NCBI (accession number KP732536). pBpuro-RnSox9 was used for stable expression studies. RnSox9 vectors tagged with hemagglutinin (HA), including wild-type HA–Sox9 and truncation mutants, were generated by PCR followed by insertion into pcDNA3.1. All cloned PCR products were verified by sequencing.

Cell culture and small molecules

The immortalized human pancreatic ductal epithelial cell line HPDE (H6c7), provided by Ming-Sound Tsao (University of Toronto, Canada), was cultured in keratinocyte serum-free (KSF) medium supplemented with bovine pituitary extract and epidermal growth factor (Life Technologies). S2-013 PDA cells were a gift of Martin Johnson (University of Alabama at Birmingham). S2-013, HEK293, 293T and RK3E cells were cultured in high-glucose DMEM supplemented with L-glutamine, penicillin, streptomycin and 10% (v/v) fetal bovine serum. Other PDA cell lines were from American Type Culture Collection (ATCC) and were cultured as recommended by ATCC. Doxycycline (Dox, 0.5 μg/ml), tetracycline (tet, 1.0 μg/ml), cycloheximide (CHX, 50 μg/ml), clasto-lactacystin β-lactone (CLβL, 10 μM) and MG132 (20 μM) were from Sigma-Aldrich.

siRNA transfection, RNA isolation and real-time quantitative PCR

siRNA target sequences are listed in supplementary material Table S2. siRNA transfection was performed using Lipofectamine RNAiMax (Life Technologies) as reported previously (Lin et al., 2011). For some experiments, the Panc-1 cells were re-transfected after 24 h. Cell extracts were prepared 48 h after the start of the initial transfection. Co-transfection of plasmids with siRNAs was as reported previously (Lin et al., 2011).

Total RNA was purified using the RNeasy Plus Mini kit (Qiagen). Reverse transcription was performed using SuperScript II (Life Technologies). Real-time quantitative (qRT)-PCR reactions utilized Brilliant II SyBr green QPCR master mix, GAPDH served as the internal control, and reactions were analyzed on an Mx3005P system (Agilent). Oligonucleotides are shown in supplementary material Table S3. qRT-PCR results represent three or more independent experiments (error bars show the s.d.).

Luciferase reporter assay

Topflash (wild-type TCF4-binding sites) or Fopflash (mutated sites) reporter constructs were gifts from Bert Vogelstein. The *Renilla* luciferase vector pRL-TK served as an internal control. For siRNA co-transfection, siRNA Ctrl2 served as the control (supplementary material Table S2). Reporter assays were performed on 12-well plates at 48 h post-transfection using Dual Luciferase Reporter Assays (Promega) as described previously (Lin et al., 2011). Data represent three or more independent experiments (error bars show the s.d.).

Protein expression studies

For immunoblotting, mouse anti-GLI1 and rabbit anti-β-TrCP, anti-SKP1 and anti-SNAI1/Snail were from Cell Signaling Technology. Rabbit anti-SOX9 was from EMD Millipore. Mouse anti-Myc (9E10) and anti-β-catenin were from BD Biosciences. Rat anti-HA (3F10) was from Roche Applied Science. Anti-MCL1 was from Santa Cruz Biotechnology (S-19).

Whole-cell lysates for immunoblotting were obtained by extraction in ice-cold RIPA buffer without SDS as described previously (Lin et al., 2011). For immunoprecipitation and co-IP, cells were resuspended in NE-A buffer and then lysed by addition of NaCl and glycerol as described previously (Chen and Bieker, 2001). GLI1 protein was precipitated with rabbit anti-GLI1 (Li et al., 2006), whereas rabbit anti-SOX9 (H-90, Santa Cruz Biotechnology) or a monoclonal anti-HA (12CA5, Roche) was used for SOX9. Normal rabbit or mouse IgG (Sigma-Aldrich) was used as a control. Protein complexes were recovered using Protein-A–Sepharose (Sigma-Aldrich).

For immunoblotting, proteins were transferred to nitrocellulose membrane and detected using chemiluminescence (Pierce ECL, Thermo-Scientific). Quantitative analysis of autoradiographic images was performed using ImageJ v1.42 (National Institutes of Health), and the normalized results were transferred to GraphPad Prism (version 5) for statistical analysis.

In vitro transformation assay

RK3E transformation assays were performed as described previously (Li et al., 2006). Cells were fixed and stained using Modified Wright Stain (Sigma-Aldrich) at 2–3 weeks post-transfection, and foci with a diameter >1.0 mm were counted.

Soft agar assay

Anchorage-independent cell growth assays were performed on six-well plates. A 2.0-ml underlay composed of 0.63% (w/v) agar in complete DMEM was placed in each well. A volume of 1.0 ml of cells (3.0×10^3) in DMEM containing 0.33% agar was plated on top. Cells were fed with 1.0 ml of 0.63% agar in DMEM each week. For induction of shRNA expression, 0.5 μg/ml of doxycycline was included. Cells were fixed after 2–3 weeks in 10% methanol/10% acetic acid and stained with 0.1% Crystal Violet (Sigma-Aldrich) in 50% methanol. Colonies >50 μm in diameter were counted under phase contrast microscopy.

Anoikis assay

Matrix deprivation assays were performed as described previously (Kumar et al., 2011). At 24 h post siRNA transfection, 2.0×10^4 cells were resuspended in 1.0 ml of complete DMEM containing 1% methylcellulose (Sigma-Aldrich) and plated in six-well low-attachment plates. Assays were performed in triplicate (error bars show the s.d.). At 24 and 48 h later, cells were collected, resuspended in Accumax (Innovative Cell Technologies) to generate single cell suspensions, and

mixed with 0.4% Trypan Blue (Cellgro). Trypan Blue staining was scored using a hemocytometer.

Spheroid formation assay

PDA cells were trypsinized, counted and suspended in six-well low-attachment plates using 1:1 DMEM/F-12 supplemented with 1× B27, 4.0 μg/ml heparin, 20 ng/ml EGF, 20 ng/ml FGF and 1% methylcellulose. For each cell line, 2000–5000 cells were plated in triplicate in a final volume of 2.0 ml. The spheroids in each well were quantified by phase contrast microscopy. For RNA isolation, spheroids were harvested after 7–10 days by centrifugation at 200 g for 1 min.

Flow cytometry

For side population analysis, cells were trypsinized, washed with PBS and resuspended in staining buffer [DMEM, 2% (v/v) FBS, 1.0 mM HEPES-KOH pH 7.0]. Samples were incubated for 30 min at 37℃ with or without 50 μg/ml verapamil (Sigma-Aldrich), mixed with Hoechst 33342 (Sigma-Aldrich) to a final concentration of 5.0 μg/ml and incubated for 90 min at 37℃ with intermittent mixing. The cells were washed twice with PBS, resuspended in sorting buffer [1×PBS, 5.0 mM EDTA, 1% (w/v) BSA, 25 mM HEPES-KOH pH 7.0], and maintained at 4℃ in the dark. Analysis was performed using a FACSAria III cell sorter (BD Biosciences), and both Hoechst Red and Hoechst Blue were measured.

Immunofluorescent staining and quantification

Cells were treated with CLβL or DMSO for 3 h before fixation. Cells were fixed and stained as described previously (Pandya et al., 2004) at 48 h post-transfection using rabbit anti-SOX9 (1:1000, EMD Millipore), mouse anti-GLI1 (1:100, Cell Signaling Technologies), anti-Myc (9E10, 2.5 μg/ml, BD Biosciences) and/or anti-β-catenin (0.17 μg/ml, BD Biosciences). Secondary antibodies were cross-absorbed Alexa-Fluor-647-conjugated goat anti-rabbit-IgG and Alexa-Fluor-555-conjugated goat anti-mouse-IgG (Life Technologies). Nuclei were counterstained in DAPI prior to mounting of coverslips using ProLong Antifade (Life Technologies).

Digital images were captured and pseudocolored using a Zeiss LSM 510 laser scanning confocal on an upright Zeiss AxioImager and Zeiss LSM software (Carl Zeiss). Images were exported as tiff files, and Corel software was used to make minor identical adjustments to the experimental and control panels in parallel. β-catenin was quantified using Image J.

Author contributions

W.D. and D.B.V. performed assays of gene expression, protein stability, protein-protein interaction and cancer stem cell properties. C.-C.L. performed some of the flow cytometry studies. K.H.M. assisted with immunofluorescence microscopy and K.M.B. assisted with flow cytometry studies. J.M.R. assisted with experimental design and the interpretation of data.

Supplementary material

Supplementary material available online at
http://jcs.biologists.org/lookup/suppl/doi:10.1242/jcs.162164/-/DC1

References

Badea, L., Herlea, V., Dima, S. O., Dumitrascu, T. and Popescu, I. (2008). Combined gene expression analysis of whole-tissue and microdissected pancreatic ductal adenocarcinoma identifies genes specifically overexpressed in tumor epithelia. *Hepatogastroenterology* **55**, 2016-2027.

Barrionuevo, F. and Scherer, G. (2010). SOX E genes: SOX9 and SOX8 in mammalian testis development. *Int. J. Biochem. Cell Biol.* **42**, 433-436.

Bhagwandin, V. J. and Shay, J. W. (2009). Pancreatic cancer stem cells: fact or fiction? *Biochim. Biophys. Acta* **1792**, 248-259.

Bhandari, R. K., Haque, M. M. and Skinner, M. K. (2012). Global genome analysis of the downstream binding targets of testis determining factor SRY and SOX9. *PLoS ONE* **7**, e43380.

Bien-Willner, G. A., Stankiewicz, P. and Lupski, J. R. (2007). SOX9cre1, a cis-acting regulatory element located 1.1 Mb upstream of SOX9, mediates its enhancement through the SHH pathway. *Hum. Mol. Genet.* **16**, 1143-1156.

Chen, X. and Bieker, J. J. (2001). Unanticipated repression function linked to erythroid Krüppel-like factor. *Mol. Cell. Biol.* **21**, 3118-3125.

Clevers, H. (2011). The cancer stem cell: premises, promises and challenges. *Nat. Med.* **17**, 313-319.

Dai, P., Akimaru, H., Tanaka, Y., Maekawa, T., Nakafuku, M. and Ishii, S. (1999). Sonic Hedgehog-induced activation of the Gli1 promoter is mediated by GLI3. *J. Biol. Chem.* **274**, 8143-8152.

Davis, M., Hatzubai, A., Andersen, J. S., Ben-Shushan, E., Fisher, G. Z., Yaron, A., Bauskin, A., Mercurio, F., Mann, M. and Ben-Neriah, Y. (2002). Pseudosubstrate regulation of the SCF$^{\beta-TrCP}$ ubiquitin ligase by hnRNP-U *Genes Dev.* **16**, 439-451.

de Crombrugghe, B., Lefebvre, V. and Nakashima, K. (2001). Regulatory mechanisms in the pathways of cartilage and bone formation. *Curr. Opin. Cell Biol.* **13**, 721-728.

Di Marcotullio, L., Ferretti, E., Greco, A., De Smaele, E., Po, A., Sico, M. A., Alimandi, M., Giannini, G., Maroder, M., Screpanti, I. et al. (2006). Numb is a suppressor of Hedgehog signalling and targets Gli1 for Itch-dependent ubiquitination. *Nat. Cell Biol.* **8**, 1415-1423.

Ding, Q., He, X., Hsu, J. M., Xia, W., Chen, C. T., Li, L. Y., Lee, D. F., Liu, J. C., Zhong, Q., Wang, X. et al. (2007). Degradation of Mcl-1 by β-TrCP mediates glycogen synthase kinase 3-induced tumor suppression and chemosensitization. *Mol. Cell. Biol.* **27**, 4006-4017.

Eberl, M., Klingler, S., Mangelberger, D., Loipetzberger, A., Damhofer, H., Zoidl, K., Schnidar, H., Hache, H., Bauer, H. C., Solca, F. et al. (2012). Hedgehog-EGFR cooperation response genes determine the oncogenic phenotype of basal cell carcinoma and tumour-initiating pancreatic cancer cells. *EMBO Mol. Med.* **4**, 218-233.

Feig, C., Gopinathan, A., Neesse, A., Chan, D. S., Cook, N. and Tuveson, D. A. (2012). The pancreas cancer microenvironment. *Clin. Cancer Res.* **18**, 4266-4276.

Feldmann, G., Dhara, S., Fendrich, V., Bedja, D., Beaty, R., Mullendore, M., Karikari, C., Alvarez, H., Iacobuzio-Donahue, C., Jimeno, A. et al. (2007). Blockade of hedgehog signaling inhibits pancreatic cancer invasion and metastases: a new paradigm for combination therapy in solid cancers. *Cancer Res.* **67**, 2187-2196.

Foster, K. W., Ren, S., Louro, I. D., Lobo-Ruppert, S. M., McKie-Bell, P., Grizzle, W., Hayes, M. R., Broker, T. R., Chow, L. T. and Ruppert, J. M. (1999). Oncogene expression cloning by retroviral transduction of adenovirus E1A-immortalized rat kidney RK3E cells: transformation of a host with epithelial features by c-MYC and the zinc finger protein GKLF. *Cell Growth Differ.* **10**, 423-434.

Frescas, D. and Pagano, M. (2008). Deregulated proteolysis by the F-box proteins SKP2 and β-TrCP: tipping the scales of cancer. *Nat. Rev. Cancer* **8**, 438-449.

Guo, W., Keckesova, Z., Donaher, J. L., Shibue, T., Tischler, V., Reinhardt, F., Itzkovitz, S., Noske, A., Zürrer-Härdi, U., Bell, G. et al. (2012). Slug and Sox9 cooperatively determine the mammary stem cell state. *Cell* **148**, 1015-1028.

Hermann, P. C., Huber, S. L., Herrler, T., Aicher, A., Ellwart, J. W., Guba, M., Bruns, C. J. and Heeschen, C. (2007). Distinct populations of cancer stem cells determine tumor growth and metastatic activity in human pancreatic cancer. *Cell Stem Cell* **1**, 313-323.

Hingorani, S. R., Wang, L., Multani, A. S., Combs, C., Deramaudt, T. B., Hruban, R. H., Rustgi, A. K., Chang, S. and Tuveson, D. A. (2005). Trp53R172H and KrasG12D cooperate to promote chromosomal instability and widely metastatic pancreatic ductal adenocarcinoma in mice. *Cancer Cell* **7**, 469-483.

Hui, C. C. and Angers, S. (2011). Gli proteins in development and disease. *Annu. Rev. Cell Dev. Biol.* **27**, 513-537.

Huntzicker, E. G. and Oro, A. E. (2008). Controlling hair follicle signaling pathways through polyubiquitination. *J. Invest. Dermatol.* **128**, 1081-1087.

Huntzicker, E. G., Estay, I. S., Zhen, H., Lokteva, L. A., Jackson, P. K. and Oro, A. E. (2006). Dual degradation signals control Gli protein stability and tumor formation. *Genes Dev.* **20**, 276-281.

Iacobuzio-Donahue, C. A., Maitra, A., Olsen, M., Lowe, A. W., van Heek, N. T., Rosty, C., Walter, K., Sato, N., Parker, A., Ashfaq, R. et al. (2003). Exploration of global gene expression patterns in pancreatic adenocarcinoma using cDNA microarrays. *Am. J. Pathol.* **162**, 1151-1162.

Ji, Z., Mei, F. C., Xie, J. and Cheng, X. (2007). Oncogenic KRAS activates hedgehog signaling pathway in pancreatic cancer cells. *J. Biol. Chem.* **282**, 14048-14055.

Jiang, J. (2006). Regulation of Hh/Gli signaling by dual ubiquitin pathways. *Cell Cycle* **5**, 2457-2463.

Kalderon, D. (2002). Similarities between the Hedgehog and Wnt signaling pathways. *Trends Cell Biol.* **12**, 523-531.

Kashimada, K. and Koopman, P. (2010). Sry: the master switch in mammalian sex determination. *Development* **137**, 3921-3930.

Kasper, M., Schnidar, H., Neill, G. W., Hanneder, M., Klingler, S., Blaas, L., Schmid, C., Hauser-Kronberger, C., Regl, G., Philpott, M. P. et al. (2006). Selective modulation of Hedgehog/GLI target gene expression by epidermal growth factor signaling in human keratinocytes. *Mol. Cell. Biol.* **26**, 6283-6298.

Kolligs, F. T., Hu, G., Dang, C. V. and Fearon, E. R. (1999). Neoplastic transformation of RK3E by mutant β-catenin requires deregulation of Tcf/Lef transcription but not activation of c-myc expression. *Mol. Cell. Biol.* **19**, 5696-5706.

Koorstra, J. B., Hustinx, S. R., Offerhaus, G. J. and Maitra, A. (2008). Pancreatic carcinogenesis. *Pancreatology* **8**, 110-125.

Kopp, J. L., von Figura, G., Mayes, E., Liu, F. F., Dubois, C. L., Morris, J. P., IV, Pan, F. C., Akiyama, H., Wright, C. V., Jensen, K. et al. (2012). Identification of Sox9-dependent acinar-to-ductal reprogramming as the principal mechanism for initiation of pancreatic ductal adenocarcinoma. *Cancer Cell* **22**, 737-750.

Kumar, S., Park, S. H., Cieply, B., Schupp, J., Killiam, E., Zhang, F., Rimm, D. L. and Frisch, S. M. (2011). A pathway for the control of anoikis sensitivity by E-cadherin and epithelial-to-mesenchymal transition. *Mol. Cell. Biol.* **31**, 4036-4051.

Lau, A. W., Fukushima, H. and Wei, W. (2012). The Fbw7 and betaTRCP E3 ubiquitin ligases and their roles in tumorigenesis. *Front. Biosci. (Landmark Ed)* **17**, 2197-2212.

Lauth, M. and Toftgård, R. (2007). Non-canonical activation of GLI transcription factors: implications for targeted anti-cancer therapy. *Cell Cycle* **6**, 2458-2463.

Lauth, M., Bergström, A., Shimokawa, T., Tostar, U., Jin, Q., Fendrich, V., Guerra, C., Barbacid, M. and Toftgård, R. (2010). DYRK1B-dependent autocrine-to-paracrine shift of Hedgehog signaling by mutant RAS. *Nat. Struct. Mol. Biol.* **17**, 718-725.

Li, X., Deng, W., Nail, C. D., Bailey, S. K., Kraus, M. H., Ruppert, J. M. and Lobo-Ruppert, S. M. (2006). Snail induction is an early response to Gli1 that determines the efficiency of epithelial transformation. *Oncogene* **25**, 609-621.

Li, C., Heidt, D. G., Dalerba, P., Burant, C. F., Zhang, L., Adsay, V., Wicha, M., Clarke, M. F. and Simeone, D. M. (2007). Identification of pancreatic cancer stem cells. *Cancer Res.* **67**, 1030-1037.

Li, S. H., Fu, J., Watkins, D. N., Srivastava, R. K. and Shankar, S. (2013). Sulforaphane regulates self-renewal of pancreatic cancer stem cells through the modulation of Sonic hedgehog-GLI pathway. *Mol. Cell. Biochem.* **373**, 217-227.

Lin, C. C., Liu, L. Z., Addison, J. B., Wonderlin, W. F., Ivanov, A. V. and Ruppert, J. M. (2011). A KLF4-miRNA-206 autoregulatory feedback loop can promote or inhibit protein translation depending upon cell context. *Mol. Cell. Biol.* **31**, 2513-2527.

Logsdon, C. D., Simeone, D. M., Binkley, C., Arumugam, T., Greenson, J. K., Giordano, T. J., Misek, D. E., Kuick, R. and Hanash, S. (2003). Molecular profiling of pancreatic adenocarcinoma and chronic pancreatitis identifies multiple genes differentially regulated in pancreatic cancer. *Cancer Res.* **63**, 2649-2657.

Lynn, F. C., Smith, S. B., Wilson, M. E., Yang, K. Y., Nekrep, N. and German, M. S. (2007). Sox9 coordinates a transcriptional network in pancreatic progenitor cells. *Proc. Natl. Acad. Sci. USA* **104**, 10500-10505.

Matheu, A., Collado, M., Wise, C., Manterola, L., Cekaite, L., Tye, A. J., Canamero, M., Bujanda, L., Schedl, A., Cheah, K. S. et al. (2012). Oncogenicity of the developmental transcription factor Sox9. *Cancer Res.* **72**, 1301-1315.

McNeill, B., Perez-Iratxeta, C., Mazerolle, C., Furimsky, M., Mishina, Y., Andrade-Navarro, M. A. and Wallace, V. A. (2012). Comparative genomics identification of a novel set of temporally regulated hedgehog target genes in the retina. *Mol. Cell. Neurosci.* **49**, 333-340.

Mills, L. D., Zhang, Y., Marler, R. J., Herreros-Villanueva, M., Zhang, L., Almada, L. L., Couch, F., Wetmore, C., Pasca di Magliano, M. and Fernandez-Zapico, M. E. (2013). Loss of the transcription factor GLI1 identifies a signaling network in the tumor microenvironment mediating KRAS oncogene-induced transformation. *J. Biol. Chem.* **288**, 11786-11794.

Morris, J. P., IV, W. a. n. g, S. C. and Hebrok, M. (2010). KRAS, Hedgehog, Wnt and the twisted developmental biology of pancreatic ductal adenocarcinoma. *Nat. Rev. Cancer* **10**, 683-695.

Murakami, S., Kan, M., McKeehan, W. L. and de Crombrugghe, B. (2000). Up-regulation of the chondrogenic Sox9 gene by fibroblast growth factors is mediated by the mitogen-activated protein kinase pathway. *Proc. Natl. Acad. Sci. USA* **97**, 1113-1118.

Nolan-Stevaux, O., Lau, J., Truitt, M. L., Chu, G. C., Hebrok, M., Fernández-Zapico, M. E. and Hanahan, D. (2009). GLI1 is regulated through

Smoothened-independent mechanisms in neoplastic pancreatic ducts and mediates PDAC cell survival and transformation. *Genes Dev.* **23**, 24-36.

Nusse, R. (2003). Wnts and Hedgehogs: lipid-modified proteins and similarities in signaling mechanisms at the cell surface. *Development* **130**, 5297-5305.

Oh, C. D., Maity, S. N., Lu, J. F., Zhang, J., Liang, S., Coustry, F., de Crombrugghe, B. and Yasuda, H. (2010). Identification of SOX9 interaction sites in the genome of chondrocytes. *PLoS ONE* **5**, e10113.

Ohlmeyer, J. T. and Kalderon, D. (1998). Hedgehog stimulates maturation of Cubitus interruptus into a labile transcriptional activator. *Nature* **396**, 749-753.

Pandya, A. Y., Talley, L. I., Frost, A. R., Fitzgerald, T. J., Trivedi, V., Chakravarthy, M., Chhieng, D. C., Grizzle, W. E., Engler, J. A., Krontiras, H. et al. (2004). Nuclear localization of KLF4 is associated with an aggressive phenotype in early-stage breast cancer. *Clin. Cancer Res.* **10**, 2709-2719.

Pasca di Magliano, M., Sekine, S., Ermilov, A., Ferris, J., Dlugosz, A. A. and Hebrok, M. (2006). Hedgehog/Ras interactions regulate early stages of pancreatic cancer. *Genes Dev.* **20**, 3161-3173.

Pei, H., Li, L., Fridley, B. L., Jenkins, G. D., Kalari, K. R., Lingle, W., Petersen, G., Lou, Z. and Wang, L. (2009). FKBP51 affects cancer cell response to chemotherapy by negatively regulating Akt. *Cancer Cell* **16**, 259-266.

Polakis, P. (1999). The oncogenic activation of β-catenin. *Curr. Opin. Genet. Dev.* **9**, 15-21.

Pritchett, J., Athwal, V., Roberts, N., Hanley, N. A. and Hanley, K. P. (2011). Understanding the role of SOX9 in acquired diseases: lessons from development. *Trends Mol. Med.* **17**, 166-174.

Rajurkar, M., De Jesus-Monge, W. E., Driscoll, D. R., Appleman, V. A., Huang, H., Cotton, J. L., Klimstra, D. S., Zhu, L. J., Simin, K., Xu, L. et al. (2012). The activity of Gli transcription factors is essential for Kras-induced pancreatic tumorigenesis. *Proc. Natl. Acad. Sci. USA* **109**, E1038-E1047.

Rhodes, D. R., Yu, J., Shanker, K., Deshpande, N., Varambally, R., Ghosh, D., Barrette, T., Pandey, A. and Chinnaiyan, A. M. (2004). ONCOMINE: a cancer microarray database and integrated data-mining platform. *Neoplasia* **6**, 1-6.

Ruiz i Altaba, A., Mas, C. and Stecca, B. (2007). The Gli code: an information nexus regulating cell fate, stemness and cancer. *Trends Cell Biol.* **17**, 438-447.

Segara, D., Biankin, A. V., Kench, J. G., Langusch, C. C., Dawson, A. C., Skalicky, D. A., Gotley, D. C., Coleman, M. J., Sutherland, R. L. and Henshall, S. M. (2005). Expression of HOXB2, a retinoic acid signaling target in pancreatic cancer and pancreatic intraepithelial neoplasia. *Clin. Cancer Res.* **11**, 3587-3596.

Seymour, P. A., Freude, K. K., Tran, M. N., Mayes, E. E., Jensen, J., Kist, R., Scherer, G. and Sander, M. (2007). SOX9 is required for maintenance of the pancreatic progenitor cell pool. *Proc. Natl. Acad. Sci. USA* **104**, 1865-1870.

Shaik, S., Nucera, C., Inuzuka, H., Gao, D., Garnaas, M., Frechette, G., Harris, L., Wan, L., Fukushima, H., Husain, A. et al. (2012). SCF(β-TRCP) suppresses angiogenesis and thyroid cancer cell migration by promoting ubiquitination and destruction of VEGF receptor 2. *J. Exp. Med.* **209**, 1289-1307.

Skaar, J. R., Pagan, J. K. and Pagano, M. (2013). Mechanisms and function of substrate recruitment by F-box proteins. *Nat. Rev. Mol. Cell Biol.* **14**, 369-381.

Stecca, B. and Ruiz I Altaba, A. (2010). Context-dependent regulation of the GLI code in cancer by HEDGEHOG and non-HEDGEHOG signals. *J. Mol. Cell Biol.* **2**, 84-95.

Sun, L., Mathews, L. A., Cabarcas, S. M., Zhang, X., Yang, A., Zhang, Y., Young, M. R., Klarmann, K. D., Keller, J. R. and Farrar, W. L. (2013). Epigenetic regulation of SOX9 by the NF-κB signaling pathway in pancreatic cancer stem cells. *Stem Cells* **31**, 1454-1466.

Taipale, J. and Beachy, P. A. (2001). The Hedgehog and Wnt signalling pathways in cancer. *Nature* **411**, 349-354.

Takahashi, K. and Yamanaka, S. (2006). Induction of pluripotent stem cells from mouse embryonic and adult fibroblast cultures by defined factors. *Cell* **126**, 663-676.

Tang, S. N., Fu, J., Nall, D., Rodova, M., Shankar, S. and Srivastava, R. K. (2012). Inhibition of sonic hedgehog pathway and pluripotency maintaining factors regulate human pancreatic cancer stem cell characteristics. *Int. J. Cancer* **131**, 30-40.

Tavella, S., Biticchi, R., Schito, A., Minina, E., Di Martino, D., Pagano, A., Vortkamp, A., Horton, W. A., Cancedda, R. and Garofalo, S. (2004). Targeted expression of SHH affects chondrocyte differentiation, growth plate organization, and Sox9 expression. *J. Bone Miner. Res.* **19**, 1678-1688.

Thayer, S. P., di Magliano, M. P., Heiser, P. W., Nielsen, C. M., Roberts, D. J., Lauwers, G. Y., Qi, Y. P., Gysin, S., Fernández-del Castillo, C., Yajnik, V. et al. (2003). Hedgehog is an early and late mediator of pancreatic cancer tumorigenesis. *Nature* **425**, 851-856.

Tian, H., Callahan, C. A., DuPree, K. J., Darbonne, W. C., Ahn, C. P., Scales, S. J. and de Sauvage, F. J. (2009). Hedgehog signaling is restricted to the stromal compartment during pancreatic carcinogenesis. *Proc. Natl. Acad. Sci. USA* **106**, 4254-4259.

Topol, L., Chen, W., Song, H., Day, T. F. and Yang, Y. (2009). Sox9 inhibits Wnt signaling by promoting β-catenin phosphorylation in the nucleus. *J. Biol. Chem.* **284**, 3323-3333.

Vidal, V. P., Chaboissier, M. C., Lützkendorf, S., Cotsarelis, G., Mill, P., Hui, C. C., Ortonne, N., Ortonne, J. P. and Schedl, A. (2005). Sox9 is essential for outer root sheath differentiation and the formation of the hair stem cell compartment. *Curr. Biol.* **15**, 1340-1351.

Vokes, S. A., Ji, H., McCuine, S., Tenzen, T., Giles, S., Zhong, S., Longabaugh, W. J., Davidson, E. H., Wong, W. H. and McMahon, A. P. (2007). Genomic

characterization of Gli-activator targets in sonic hedgehog-mediated neural patterning. *Development* **134**, 1977-1989.

Wan, M., Tang, Y., Tytler, E. M., Lu, C., Jin, B., Vickers, S. M., Yang, L., Shi, X. and Cao, X. (2004). Smad4 protein stability is regulated by ubiquitin ligase SCF$^{\beta\text{-TrCP1}}$. *J. Biol. Chem.* **279**, 14484-14487.

Wang, H., McKnight, N. C., Zhang, T., Lu, M. L., Balk, S. P. and Yuan, X. (2007). SOX9 is expressed in normal prostate basal cells and regulates androgen receptor expression in prostate cancer cells. *Cancer Res.* **67**, 528-536.

Wang, H., Leav, I., Ibaragi, S., Wegner, M., Hu, G. F., Lu, M. L., Balk, S. P. and Yuan, X. (2008). SOX9 is expressed in human fetal prostate epithelium and enhances prostate cancer invasion. *Cancer Res.* **68**, 1625-1630.

Weinberg, R. A. (2007). Growth factors, receptors, and Cancer. In *The Biology of Cancer* (ed. R. A. Weinberg), pp. 119-158. New York, NY: Garland Science, Taylor and Francis Group, LLC.

Zhou, B. P., Deng, J., Xia, W., Xu, J., Li, Y. M., Gunduz, M. and Hung, M. C. (2004). Dual regulation of Snail by GSK-3beta-mediated phosphorylation in control of epithelial-mesenchymal transition. *Nat. Cell Biol.* **6**, 931-940.